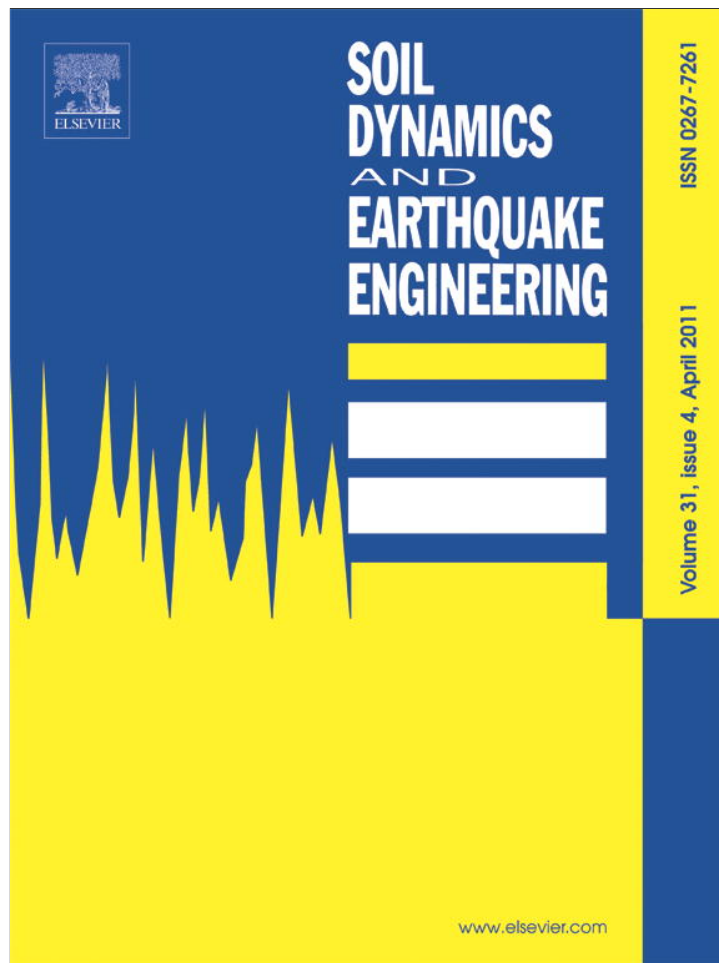


Provided for non-commercial research and education use.
Not for reproduction, distribution or commercial use.



This article appeared in a journal published by Elsevier. The attached copy is furnished to the author for internal non-commercial research and education use, including for instruction at the authors institution and sharing with colleagues.

Other uses, including reproduction and distribution, or selling or licensing copies, or posting to personal, institutional or third party websites are prohibited.

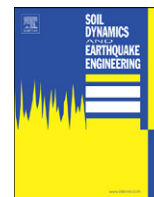
In most cases authors are permitted to post their version of the article (e.g. in Word or Tex form) to their personal website or institutional repository. Authors requiring further information regarding Elsevier's archiving and manuscript policies are encouraged to visit:

<http://www.elsevier.com/copyright>



Contents lists available at ScienceDirect

Soil Dynamics and Earthquake Engineering

journal homepage: www.elsevier.com/locate/soildyn

A ground motion selection and modification method capturing response spectrum characteristics and variability of scenario earthquakes

Gang Wang*

Department of Civil and Environmental Engineering, Hong Kong University of Science and Technology, Clear Water Bay, Kowloon, Hong Kong

ARTICLE INFO

Article history:

Received 9 July 2010

Received in revised form

26 October 2010

Accepted 24 November 2010

Available online 22 December 2010

ABSTRACT

Earthquake ground motion variability is one of the primary sources of uncertainty in the assessment of the seismic performance of civil systems. The paper presents a novel method to select and modify ground motions to achieve specified response spectrum variability. The resulted ground motions capture the median, standard deviation and correlations of response spectra of an earthquake scenario conditioned on a specified earthquake magnitude, source-to-site distance, fault mechanism, site condition, etc.

The proposed method was evaluated through numerical analyses of a 20-story RC frame structure. The example demonstrated the excellent capacity of the proposed method in capturing the full distribution of nonlinear structural responses under a specified scenario. In particular, a suite of 30 or 60 records selected using the refined algorithm can lead to statistically stable results similar to those obtained from a much larger set. The proposed algorithm is computationally efficient. It shows great potential in the performance-based earthquake design of nonlinear civil systems.

© 2010 Elsevier Ltd. All rights reserved.

1. Introduction

In recent years, time-history analyses have become more frequently used in earthquake design of civil infrastructure. Researchers and practitioners generally agree that earthquake ground motion variability is one of the major sources of uncertainty in the assessment of the seismic performance of the civil systems. Due to the lack of recorded time histories at design levels, which are usually rare events, it is critical to develop systematic methods to select from existing ground motion time histories and modify them to realistically represent important aspects of the design earthquakes. Although many ground motion selection and modification (GMSM) methods exist, consensus has not yet been reached regarding the accuracy and performance of these methods.

Since traditionally the seismic hazard at a site has been represented by design spectra for design purposes, most existing GMSM models mainly focus on developing time-history datasets that, in aggregate, have response spectra resembling a specified target spectrum. Sometimes, modifications to existing ground motion time histories are necessary in order to better fit the specified spectral shape, including the use of the “amplitude-scaling” approach to scale the amplitude of time histories to achieve an averaged fit to a target spectrum [1], or “spectrum-matching” approaches to adjust the ground motion time histories either in the time domain or in the frequency domain so that the

modified response spectrum is closely matched to the design spectrum (e.g. [2,3]). Each approach has its advantages and appears to be a generally acceptable method in engineering practice. Furthermore, methods focusing on other response characteristics of the nonlinear system, such as a proxy response or inelastic displacement, have also been pursued by some researchers (e.g. [4,5]). A state-of-the-art review of earthquake ground motion selection methods for structural evaluation can be found in [6].

Motivated by the need to reduce the number of records required for dynamic analyses, current GMSM efforts mainly aim at developing a suite of time histories that minimizes the dispersion in predicting the median response of the systems. For example, for a first-mode dominated structure, time histories scaled to match the target spectrum at the period of the first mode of the structure can yield a good estimate of the median structural response [7]. On the other hand, performance-based design requires seismic performance evaluation at all hazard levels. Therefore, it is important to capture the record-to-record ground motion variability in time-history analyses in an effective and realistic manner. To date, only limited works were conducted to consider the ground motion variability in record selection procedures. The recent ATC-58 guideline [8] recommended selecting eleven ground motion records randomly from a chosen magnitude and distance bin and then scaling them to match the target spectrum amplitude at the fundamental period of the structure. However, the random nature of the selection procedure makes it unreliable to represent the true ground motion variability. A semi-automated method recently proposed by Kottke and Rathje [9] is also worth mentioning. Their method aims at selecting and modifying a suite of ground motions to match a specified median

* Tel.: +852 2358 7161; fax: +852 2358 1534.

E-mail address: gwang@ust.hk

target spectrum and the standard deviation of the spectral amplitudes at the same time. The semi-automated method scales the records in two steps: first, each record is scaled by an average scale factor to achieve an overall fit to the median target spectrum; then, each record is re-scaled to modify the standard deviation within the set. However, this method overlooks the correlation structure (covariance) of the spectral distribution over different periods. Therefore, the procedure generates ground motion datasets whose spectral shapes resemble that of the median target spectrum.

For a more realistic representation of the record-to-record response spectrum variability, a novel GSM method is proposed in this paper. The method selects a suite of ground motion time histories that captures the median, the standard deviation and the correlation structure of the spectral distribution, given a specified earthquake magnitude, distance, site condition, etc. The consistency and convergence properties of the proposed GSM method will then be examined. A refined algorithm is proposed to improve the efficiency and accuracy of the algorithm. Preliminary evaluation of the method is conducted through nonlinear analysis of a tall building. Implications of the new method in performance-based earthquake engineering will be discussed in the conclusion.

2. Response spectrum variability

Before proceeding to the GSM method, we examine the response spectrum variability of a scenario earthquake. The scenario is defined as conditioned on a specified earthquake magnitude, source-to-site distance, fault mechanism, site condition and other parameters. Analyses of ground motion dataset demonstrated that the statistical distribution of spectral accelerations of individual periods can be well approximated by lognormal distributions for a given earthquake scenario. Empirical predictive equations for the mean and the standard deviation of $\ln S_a$ (the natural logarithm of spectral accelerations) for a scenario earthquake can be obtained from ground motion attenuation models (e.g. [10–12]). As shown in Fig. 1(a), the predicted median spectral acceleration (which equals the exponential of the mean $\ln S_a$) is usually a smooth curve, and it

does not represent the response spectrum of any actual ground motion. Instead, individual response spectrum shows variability in spectral amplitudes over different periods. The correlation between the spectral values of different periods was found to be an intrinsic property of ground motions [13]. It can be calculated from a set of response spectra using the following formulation:

$$\rho_{\ln S_a(T_1), \ln S_a(T_2)} = \frac{\sum_{i=1}^N (\ln S_a^{(i)}(T_1) - \overline{\ln S_a(T_1)}) (\ln S_a^{(i)}(T_2) - \overline{\ln S_a(T_2)})}{\sqrt{\sum_{i=1}^N (\ln S_a^{(i)}(T_1) - \overline{\ln S_a(T_1)})^2 \sum_{i=1}^N (\ln S_a^{(i)}(T_2) - \overline{\ln S_a(T_2)})^2}} \quad (1)$$

where N is the number of records, $\ln S_a^{(i)}(T_1)$ is the $\ln S_a$ of i th record evaluated at period T_1 and $\overline{\ln S_a(T_1)}$ is the mean value of $\ln S_a(T_1)$ of all N records.

Based on regression analyses of a strong motion dataset, empirical correlation coefficient between the spectral values of different periods can be expressed as follows [14]:

$$\rho_{\ln S_a(T_1), \ln S_a(T_2)} = \begin{cases} \text{if } T_{\max} < 0.109 & C_2 \\ \text{else if } T_{\min} > 0.109 & C_1 \\ \text{else if } T_{\max} < 0.2 & \min(C_2, C_4) \\ \text{else} & C_4 \end{cases} \quad (2)$$

where

$$C_1 = 1 - \cos\left(\frac{\pi}{2} - 0.366 \ln\left(\frac{T_{\max}}{\max(T_{\min}, 0.109)}\right)\right)$$

$$C_2 = \begin{cases} 1 - 0.105(1 - 1/(1 + e^{100T_{\max} - 5})) \left(\frac{T_{\max} - T_{\min}}{T_{\max} - 0.0099}\right) & \text{if } T_{\max} < 0.2 \\ 0 & \text{otherwise} \end{cases}$$

$$C_3 = \begin{cases} C_2 & \text{if } T_{\max} < 0.109 \\ C_1 & \text{otherwise} \end{cases}$$

$$C_4 = C_1 - 0.5(\sqrt{C_3} - C_3) \left(1 + \cos\left(\frac{\pi T_{\min}}{0.109}\right)\right)$$

$T_{\min} = \min(T_1, T_2)$ and $T_{\max} = \max(T_1, T_2)$

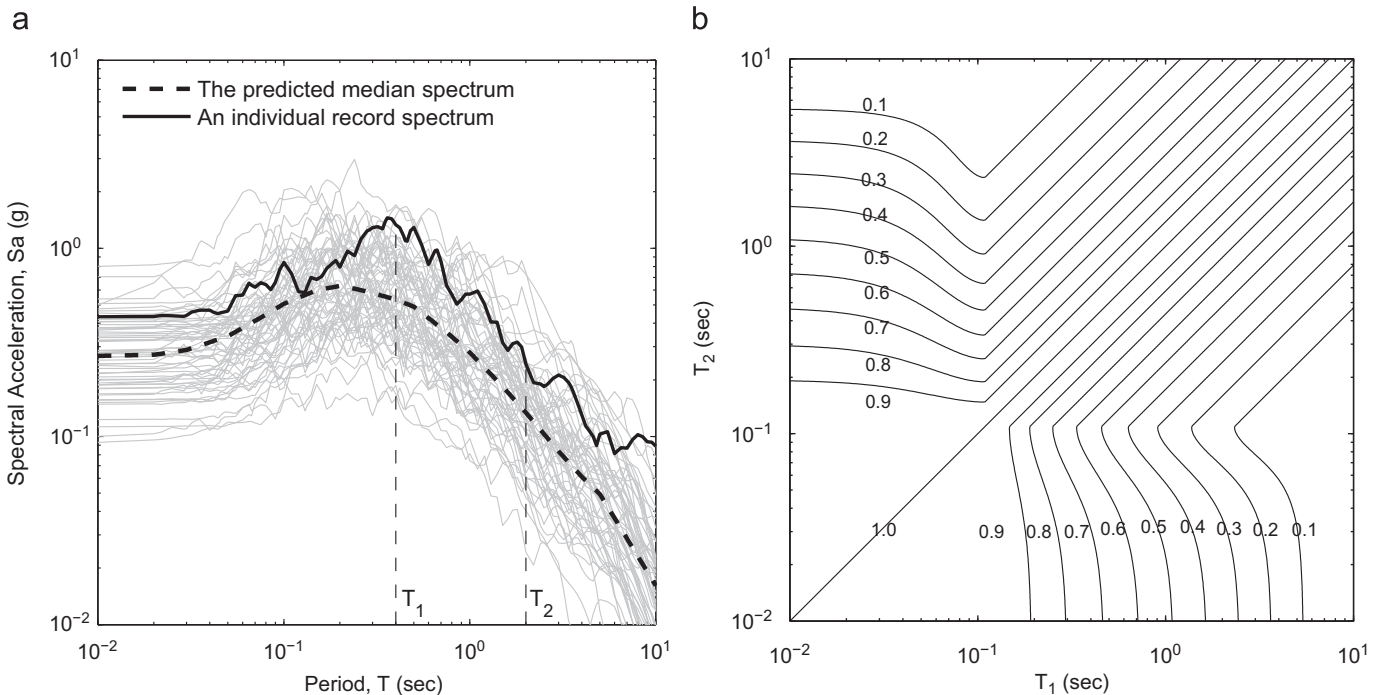


Fig. 1. Example of response spectrum variability and correlation. (a) Spectral acceleration variability, (b) Correlation coefficient of spectral accelerations.

The above expression is illustrated in Fig. 1(b). The formulation is valid over a period range of 0.01–10 s. The resulting covariance matrix is a symmetric positive definite matrix, which allows

for random sample generation. As will be discussed later, this property is important for the proposed ground motion selection procedure.

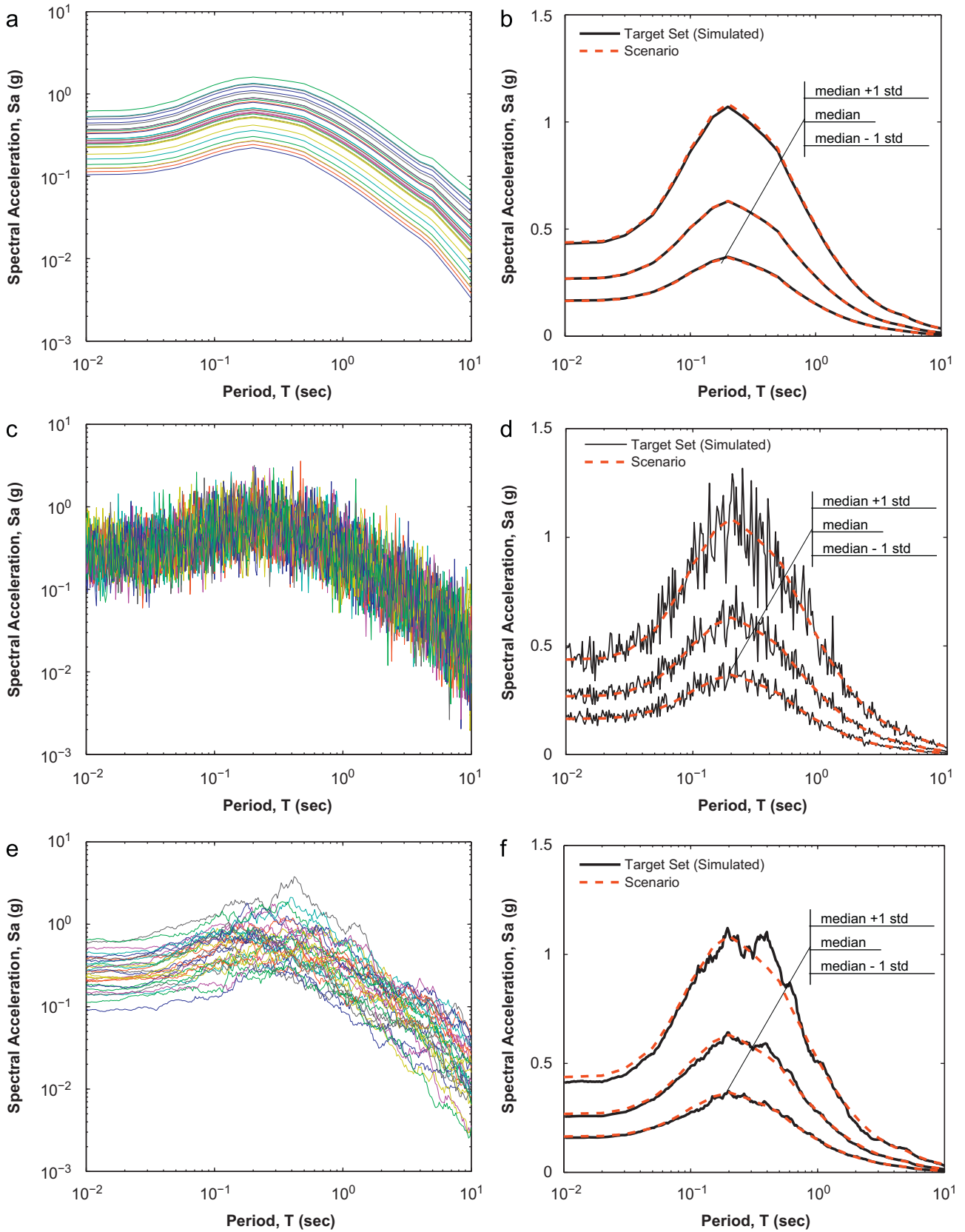


Fig. 2. Distribution of response spectra: (a, b) perfect correlation, (c, d) zero correlation, and (e, f) empirical correlation.

Fig. 2 illustrates the importance of the spectral correlation in controlling the response spectrum variability of a ground motion dataset. In an extreme case where the spectral values are assumed to be perfectly correlated (let $\rho=1$ for all period pairs), the numerically simulated spectra are a set of parallel lines, as shown in Fig. 2(a). Although the median and standard deviation of the simulated target set closely resemble the statistical distribution of a scenario response spectrum shown in Fig. 2(b), obviously, the set of perfectly correlated records cannot represent the true spectral variability of the ground motion. Similarly, a set of ground motions with zero spectral correlation (let $\rho=0$ for all period pairs) can also fit reasonably well to the median and standard deviation curves of the scenario response spectrum, as shown in Fig. 2(c) and (d), the spectral distribution cannot possibly represent any real earthquake scenario. More realistic representation of the spectral variability can be simulated using the smoothed empirical correlation Eq. (2), as shown in Fig. 2(e) and (f). Therefore, in order to realistically represent the response spectrum variability, the selected ground motion dataset should preserve the median, the standard deviation of the spectral distribution, and more importantly, the correlation structure between the spectral values of different periods. Accordingly, the median, the standard deviation and the correlation structure are termed as the “response spectrum variability vector” of the ground motion.

3. Ground motion dataset

The database used in this study was derived from the Pacific Earthquake Engineering Research Center (PEER) Next-Generation Attenuation (NGA) strong motion database (<http://peer.berkeley.edu/nga/>), which was coordinated by the PEER-Lifelines Program (PEER-LL), in partnership with the U.S. Geological Survey (USGS) and the Southern California Earthquake Center (SCEC) [15–17]. The original PEER-NGA database includes 3551 three-component recordings from 173 earthquakes obtained by 1456 recording stations. Based on seismological information, the horizontal components of each recording have been rotated to fault normal (FN) and fault parallel (FP) directions, together with the corresponding vertical ground motion time histories. The original PEER-NGA database was thoroughly reviewed to form an updated database. A record is excluded from the updated database if (a) it was considered to be from tectonic environments other than shallow crustal earthquakes in active tectonic regions, e.g. a record from subduction zones, (b) the earthquake was poorly defined, (c) the conditions, under which the record was obtained, were not considered to be sufficiently close to free-field ground surface conditions, e.g. a record obtained in a basement or on the ground floor of a tall building, (d) there was an absence of information on soil/geologic conditions at the recording station, (e) it had only one horizontal component, (f) it had not been rotated to FN and FP directions because of an absence of information on sensor orientations or fault strike, or (g) it was proprietary data. In total, 369 records were excluded from the original PEER-NGA dataset, leaving 3182 three-component records in the updated database. The updated database can better represent shallow crustal earthquakes in active tectonic regions. The magnitude and distance distribution of the records are illustrated in Fig. 3. It is noted that the updated database has been used to develop the Design Ground Motion Library (DGML) by the author and coworkers [1].

For each record, comprehensive ground motion parameters were compiled or estimated through the PEER-NGA effort. Besides the response spectrum, the ground motion characteristics that are important to the seismic response of the facility should also be considered in the GMSM scheme. These include the range of earthquake magnitude, the types of faulting, the range of the

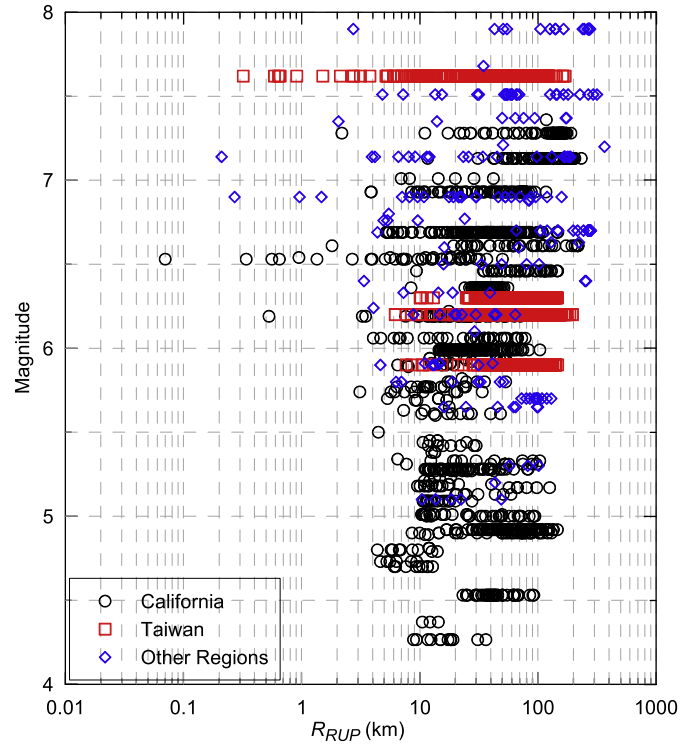


Fig. 3. Magnitude and rupture distance (R_{rup}) distribution of the updated PEER-NGA strong motion database.

closest distance measures from earthquake source to recording stations (e.g. rupture distance, Joyner–Boore distance, etc.), local site conditions at recording stations (e.g. the range of average shear wave velocity in the upper 30 m of sediments, V_{s30}), the range of significant duration, presence or absence of strong velocity pulses, among other characteristics. These characteristics, along with the spectral accelerations, need to be considered in the ground motion selection and modification process.

4. Ground motion selection and modification method

4.1. The algorithm

Finding the optimal combination of a set of N records and their corresponding scale factors to best approximate the prescribed response spectrum variability of a scenario earthquake is by no means an easy task. For example, setting aside the scale factors, there are about 3×10^{18} possible combinations to select a set of 7 records out of a database of 1500. The number of combinations explodes to a staggering 1.5×10^{158} if the attempt is to select 100 records out of a database of the same size. Therefore, a mathematically rigorous solution to this problem is not feasible at this moment. Instead, this paper presents a computationally efficient algorithm based on random generation of the target spectra following a specified statistical distribution. The algorithm is described in the following steps:

4.1.1. Step (1). Develop the target spectrum set

The response spectrum can be written as a vector of n scalar variables, denoted as $[\ln S_a(T_1), \ln S_a(T_2), \dots, \ln S_a(T_n)]$. Each variable follows normal distribution whose mean and the standard deviation can be obtained from an empirical ground motion attenuation model for a specified scenario (e.g. [10–12]). The correlation coefficient between two variables, $\rho_{\ln S_a(T_i), \ln S_a(T_j)}$, can be obtained via Eq. (2). A suite of target spectra can be obtained by random

sampling from a multivariate normal distribution with the following specified mean and covariance matrices:

$$\ln S_a^{\text{target}} = \mathcal{N}(\boldsymbol{\mu}_{\ln S_a}, \boldsymbol{\Sigma}_{\ln S_a}) \quad (3)$$

where $\boldsymbol{\mu}_{\ln S_a}$ represents the mean of the vector $[\ln S_a(T_1), \ln S_a(T_2), \dots, \ln S_a(T_n)]$, i.e.

$$\boldsymbol{\mu}_{\ln S_a} = [\mu_{\ln S_a(T_1)}, \mu_{\ln S_a(T_2)}, \dots, \mu_{\ln S_a(T_n)}] \quad (4)$$

and $\boldsymbol{\Sigma}_{\ln S_a}$ is the covariance matrix of the vector $[\ln S_a(T_1), \ln S_a(T_2), \dots, \ln S_a(T_n)]$. It can be written as

$$\boldsymbol{\Sigma}_{\ln S_a} = \begin{bmatrix} (\sigma_{\ln S_a(T_1)})^2 & \rho_{\ln S_a(T_1), \ln S_a(T_2)} \sigma_{\ln S_a(T_1)} \sigma_{\ln S_a(T_2)} & \dots & \rho_{\ln S_a(T_1), \ln S_a(T_n)} \sigma_{\ln S_a(T_1)} \sigma_{\ln S_a(T_n)} \\ \rho_{\ln S_a(T_2), \ln S_a(T_1)} \sigma_{\ln S_a(T_2)} \sigma_{\ln S_a(T_1)} & (\sigma_{\ln S_a(T_2)})^2 & \dots & \rho_{\ln S_a(T_2), \ln S_a(T_n)} \sigma_{\ln S_a(T_2)} \sigma_{\ln S_a(T_n)} \\ \dots & \dots & \dots & \dots \\ \rho_{\ln S_a(T_n), \ln S_a(T_1)} \sigma_{\ln S_a(T_n)} \sigma_{\ln S_a(T_1)} & \rho_{\ln S_a(T_n), \ln S_a(T_2)} \sigma_{\ln S_a(T_n)} \sigma_{\ln S_a(T_2)} & \dots & (\sigma_{\ln S_a(T_n)})^2 \end{bmatrix} \quad (5)$$

Matlab function *mvnrand* was used to randomly sample a suite of N target spectra following the distribution defined in Eq. (3). Seeds for random number generation can be specified in order to produce repeatable results. Accordingly, the so-called target residuals are defined as follows to measure the differences between the specified mean, standard deviation and correlation coefficient with these obtained from the suite of target spectra:

$$\begin{aligned} \mathcal{R}_1 &= \sum_{i=1}^n w(T_i) [\mu_{\ln S_a^{\text{target}}(T_i)} - \mu_{\ln S_a(T_i)}]^2 / \sum_{i=1}^n w(T_i) \\ \mathcal{R}_2 &= \sum_{i=1}^n w(T_i) [\sigma_{\ln S_a^{\text{target}}(T_i)} - \sigma_{\ln S_a(T_i)}]^2 / \sum_{i=1}^n w(T_i) \\ \mathcal{R}_3 &= \sum_{i=1}^n \sum_{j=1}^n w(T_i) w(T_j) \\ &\quad \times [\rho_{\ln S_a^{\text{target}}(T_i), \ln S_a^{\text{target}}(T_j)} - \rho_{\ln S_a(T_i), \ln S_a(T_j)}]^2 / \sum_{i=1}^n w(T_i) \sum_{j=1}^n w(T_j) \end{aligned} \quad (6)$$

Throughout the paper, discrete spectral periods $[T_1, T_2, \dots, T_n]$ are specified as evenly spaced in log space, with 100 points per decade. Therefore, a total of 301 spectral periods are used to cover the period range of 0.01–10 s. The weight functions $w(T_i)$ in Eqs. (6), (8), (9) and (11) allow relative weights to be assigned to different parts of the period range of interest. Therefore, they provide greater flexibility to the selection procedure. For simplicity, an equal weight will be used for all spectral periods ranging from 0.01 to 10 s in the examples used in the paper.

In principal, there are many ways to define a total target residual as the metric to evaluate the overall fitness of the generated target spectra to the specified scenario. One plausible formulation is to define the total target residual as a linear combination of \mathcal{R}_1 and \mathcal{R}_2 :

$$\mathcal{R}_{\text{target}} = a\mathcal{R}_1 + b\mathcal{R}_2 \quad (7)$$

Note that the correlation coefficients are already approximately prescribed in each multivariable generation process in the first place; therefore, the residual \mathcal{R}_3 is not explicitly included in the total residual formulation of Eq. (7). Since the objective of the proposed method is to capture the spectral variability, matching the target median and the standard deviation to the specified values is regarded as equally important. Therefore, a practical approach is to assign both a and b to 1.

By repeating step (1) for a limited number of times (300 times based on tests), one can identify a set of N spectra that yields the smallest total target residual via Eq. (7). The set is called the

“optimal target spectrum set”, which will be used later on in the selection and scaling of the record set.

4.1.2. Step (2). Specify the search criterion and limits for searches

Besides the spectral shape, the ground motion characteristics that are important to the time-history response of the civil systems may also include the number of strong shaking cycles, the shaking duration, the near-field directivity effects, pulse sequencing, etc. Limits and restrictions on the searches may include the range of earthquake magnitudes, the type of faulting, the range of distances,

the range of V_{S30} , the range of significant durations, whether records are to exclude, include or be limited to pulse records, limits on the scale factor f and restrictions on directional component (i.e., arbitrary FN or FP components, FN components only, FP component only, or FN and FP components in pair). The screening process will reduce the ground motion database to a smaller selection bin.

4.1.3. Step (3). Find the scaled record set that best matches the target set

For each target spectrum obtained in step (1), each record within the selection bin is linearly scaled. To identify the one that can render the closest match to the target spectrum, the weighted sum of squared errors (WSSE) between the logarithms of the target spectrum and the scaled record spectrum is used:

$$\text{WSSE} = \sum_{i=1}^n w(T_i) [\ln(S_a^{\text{target}}(T_i)) - \ln(f S_a^{\text{record}}(T_i))]^2 \quad (8)$$

where the parameter $w(T_i)$ is a weight function to assign the relative weights to period T_i , which can be in the same form as that in Eq. (6). Parameter f in the above equation is a (positive) linear scale factor applied to the entire response spectrum of the recording. Given the target and the unscaled record spectra, WSSE is a quadratic function of the scale factor f and it admits a global minimum. Accordingly, the optimal scale factor f^* can be determined by minimizing the WSSE:

$$\ln f^* = \frac{\sum_{i=1}^n w(T_i) \ln(S_a^{\text{target}}(T_i) / S_a^{\text{record}}(T_i))}{\sum_{i=1}^n w(T_i)} \quad (9)$$

If weights are assigned equally to all periods of interests, the above expression reduces to

$$\ln f^* = \frac{1}{n} \sum_{i=1}^n \ln f(T_i) = \frac{1}{n} \sum_{i=1}^n \ln(S_a^{\text{target}}(T_i) / S_a^{\text{record}}(T_i)) \quad (10)$$

The above equation admits a simple mathematical interpretation: the optimal scale factor f^* is the geometric mean of the scale factors $f(T_i) = S_a^{\text{target}}(T_i) / S_a^{\text{record}}(T_i)$ of different periods.

The WSSE value for the scaled record can be obtained by substituting Eq. (9) back into Eq. (8). Similarly, WSSEs are calculated for all records in the selection bin. The scaled record that gives the minimal WSSE is the one that best matches the spectral shape of the target spectrum over the specified period range of interest among all records in the selection bin. Fig. 4 illustrates an example of such a scaled record and the target spectrum. Note that the amplitude scaling only linearly translates the shape of a spectrum

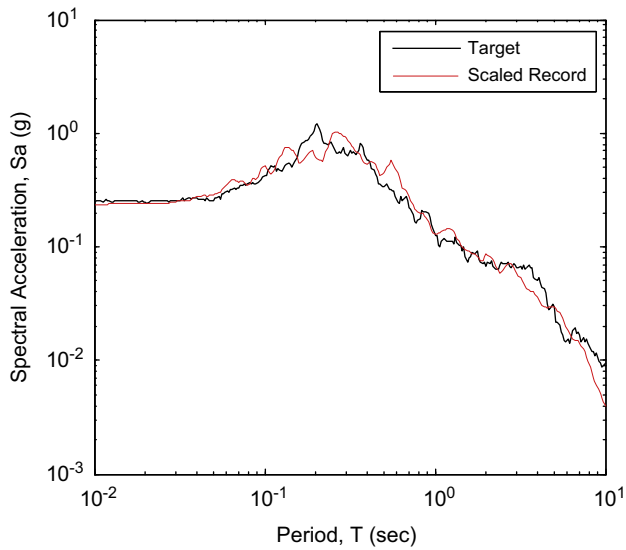


Fig. 4. Example of a scaled record spectrum that best matches the target spectrum.

in a logarithmic scale, and thus the relative frequency content of the original record will not be changed. The process is repeated for each target spectrum until a set of N scaled records is obtained. The collection, $S_a^{\text{scaled}} = \cup (f^* S_a^{\text{record}^*})$, is called “the selected record set”.

The above procedure is easy to implement, and it remains flexible to incorporate other features such as specifying the desirable scale factor range to avoid excessive scaling, or specifying the selected record from different recordings, etc. In practice, one may prefer that the selected records are derived from distinctive ground motion records. It is easy to avoid repetition by eliminating the selected record one by one from the selection bin after it was selected in step (3).

4.1.4. Step (4). Evaluate the selected record set

In this step, the response spectrum variability vector of the selected (scaled) records is calculated and compared with the prescribed values to define the so-called record residuals, similar to Eq. (6):

$$\mathcal{R}_1 = \frac{\sum_{i=1}^n w(T_i) [\mu_{\ln S_a^{\text{scaled}}}(T_i) - \mu_{\ln S_a}(T_i)]^2}{\sum_{i=1}^n w(T_i)}$$

$$\mathcal{R}_2 = \frac{\sum_{i=1}^n w(T_i) [\sigma_{\ln S_a^{\text{scaled}}}(T_i) - \sigma_{\ln S_a}(T_i)]^2}{\sum_{i=1}^n w(T_i)}$$

Table 1
Ground motion selection and modification algorithm.

1. Generate a set of N target spectra following lognormal distribution with the specified mean vector $\mu_{\ln S_a}$ and covariance matrix $\Sigma_{\ln S_a}$ of the natural log of spectral acceleration: $\ln S_a^{\text{target}} = \mathcal{N}(\mu_{\ln S_a}, \Sigma_{\ln S_a})$
2. Compute the total residuals of the generated target set:

$$\mathcal{R}_1 = \frac{\sum_{i=1}^n w(T_i) [\mu_{\ln S_a^{\text{target}}}(T_i) - \mu_{\ln S_a}(T_i)]^2}{\sum_{i=1}^n w(T_i)}$$

$$\mathcal{R}_2 = \frac{\sum_{i=1}^n w(T_i) [\sigma_{\ln S_a^{\text{target}}}(T_i) - \sigma_{\ln S_a}(T_i)]^2}{\sum_{i=1}^n w(T_i)}$$

$$\mathcal{R}_{\text{target}} = \mathcal{R}_1 + \mathcal{R}_2.$$
3. Repeat steps 1–2 for m times ($m = 300$ is recommended).
4. Choose the optimal target set that minimizes $\mathcal{R}_{\text{target}}$.
5. Specify the search criterion and limits (e.g. limits for earthquake magnitudes, distances, duration, scale factors, etc.) to reduce the strong motion database to a selection bin.
6. For each target spectrum vector $[S_a^{\text{target}}(T_1), S_a^{\text{target}}(T_2), \dots, S_a^{\text{target}}(T_n)]$ in the optimal target set, do
 - 6.1. For each record spectrum vector $[S_a^{\text{record}}(T_1), S_a^{\text{record}}(T_2), \dots, S_a^{\text{record}}(T_n)]$ in the selection bin, do
 - 6.1.1. Compute the scale factor

$$\ln f^* = \frac{\sum_{i=1}^n w(T_i) \ln(S_a^{\text{target}}(T_i) / S_a^{\text{record}}(T_i))}{\sum_{i=1}^n w(T_i)}$$
 - 6.1.2. Compute the weighted sum of squared errors (WSSE)

$$\text{WSSE} = \sum_{i=1}^n w(T_i) [\ln(S_a^{\text{target}}(T_i)) - \ln(f^* S_a^{\text{record}}(T_i))]^2$$
- End
- 6.2. Identify the record spectrum $S_a^{\text{record}^*}$ and scale factor f^* that minimize WSSE.
- 6.3. **Optional:** Remove the record selected in 6.2 from the selection bin to avoid repetition.
- End
7. Assemble the scaled record set from Step 6: $S_a^{\text{scaled}} = \cup (f^* S_a^{\text{record}^*})$
8. Compute the residuals of the scaled record set:

$$\mathcal{R}_1 = \frac{\sum_{i=1}^n w(T_i) [\mu_{\ln S_a^{\text{scaled}}}(T_i) - \mu_{\ln S_a}(T_i)]^2}{\sum_{i=1}^n w(T_i)},$$

$$\mathcal{R}_2 = \frac{\sum_{i=1}^n w(T_i) [\sigma_{\ln S_a^{\text{scaled}}}(T_i) - \sigma_{\ln S_a}(T_i)]^2}{\sum_{i=1}^n w(T_i)}.$$

Compute the total record residual: $\mathcal{R}_{\text{record}} = \mathcal{R}_1 + \mathcal{R}_2$
9. Inspect the selected record set. If necessary, go back to Step 5 to change the search criterion and limits.
10. The refined algorithm
 - 10.1. Do steps 1–3, get m sets of N target spectrum and their $\mathcal{R}_{\text{target}}$.
 - 10.2. Compute threshold $\delta = \exp(\mu(\ln \mathcal{R}_{\text{target}}) - \sigma(\ln \mathcal{R}_{\text{target}}))$.
 - 10.3. For each target spectra set whose $\mathcal{R}_{\text{target}} \leq \delta$, do Steps 5–9.
 - End
 - 10.4. Choose the scaled record set that minimizes the total record residual $\mathcal{R}_{\text{record}}$.

$$\mathcal{R}_3 = \sum_{i=1}^n \sum_{j=1}^n w(T_i)w(T_j) \times \left[\rho_{\ln S_a^{\text{scaled}}(T_i), \ln S_a^{\text{scaled}}(T_j)} - \rho_{\ln S_a(T_i), \ln S_a(T_j)} \right]^2 \bigg/ \sum_{i=1}^n w(T_i) \sum_{j=1}^n w(T_j) \quad (11)$$

Similarly, the total record residual is defined as

$$\mathcal{R}_{\text{record}} = \mathcal{R}_1 + \mathcal{R}_2 \quad (12)$$

The total record residual can be used to evaluate the quality of the selected records. In Section 4.3, a refined algorithm will be proposed to search the record set that yields a global minimum of the total record residual among all realizations.

Steps (1)–(4) result in a set of N scaled records that best matches the optimal target spectrum set individually. It is worth pointing out that the proposed algorithm is simple and fast, and the complexity of the algorithm is linear with respect to the size of the selected record (N) and the size of the database (K), i.e., the complexity is $O(N \times K)$. It only takes less than 2 min on a personal computer to complete the searching and scaling of 30 records from a database of about 7000 records. For clarity, the above algorithm is also outlined in Table 1.

4.2. Consistency and convergence of the algorithm

In this section, two important properties of the proposed algorithm will be further investigated:

- (1) Consistency: Will a target set with a smaller residual necessarily result in a scaled record set with a smaller residual?
- (2) Convergence: How many random samplings of the target set are sufficient to result in a scaled record set with a sufficiently small residual? What sample size (i.e. record population) would be sufficient to represent the spectral variability?

To test the consistency and convergence of the proposed algorithm, ground motion sets were selected independently from

the updated PEER-NGA database based on the proposed procedure. The response spectra represent ground motions associated with a specified scenario earthquake (magnitude $M_w=7$, strike-slip faulting, rupture distance $\mathcal{R}_{rup} = 10\text{km}$ and the average of shear wave velocity in the first 30 m of the site $V_{s30}=400\text{ m/s}$). The median response spectrum and the standard deviation were determined using the Campbell and Bozorgnia attenuation model [10], and the correlation coefficients were from [14].

Following Section 4.1 Step (1), target spectra sets with population size of 30, 60, 100 and 200 were randomly sampled 300 times for each population. Accordingly, record sets were selected and scaled using each target set. The target residuals and the record residuals were calculated via Eqs. (7) and (12), and the pairs of residuals were plotted in Fig. 5. It is observed that the total residuals of the target set versus the record set generally follow a linear trend, while the record residuals are usually slightly larger than the target residuals. For each population case, a target set with a smaller residual is more likely to result in a selected set with a smaller residual. However, the target set with the minimum residual (called the optimal target set) does not necessarily correspond to the record set with the minimum residual. Therefore, the residual of records selected according to the optimal target set may not be the global minimum.

It is also interesting to examine the statistical distributions of the target residuals and record residuals. Fig. 6(a) shows the cumulative distribution functions (CDFs) of the residuals for each population case. It is observed that all target residuals and record residuals approximately follow lognormal distributions since their CDFs can be well approximated by lognormal CDFs. The record residual CDF of the population 30 case approximately coincides with the target residual CDF, while the record residuals of the population 200 case have a higher median and a smaller standard deviation (in log space) than those of the target residual distribution. Increasing the population size reduces the minimum residual as the data clusters shift to the left-hand side in Fig. 5. Also, the CDFs of both target residuals and record residuals in Fig. 6(a) shift to the left when the population size increases. However, the benefit of increasing population size from 100 to 200 is not pronounced comparing these two cases.

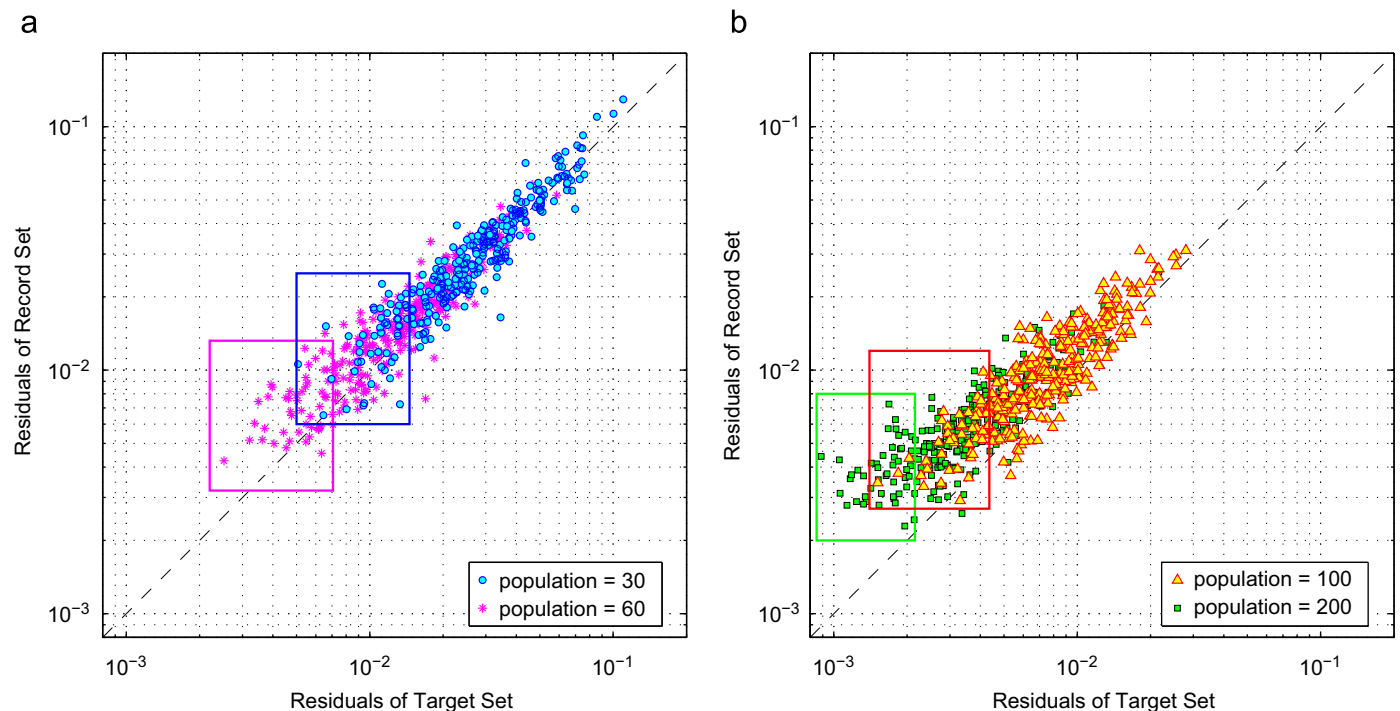


Fig. 5. Residuals of the target set versus the record set (unit: g^2). Note: Each box highlights the subset of data points that are included using the refined search algorithm.

Section 4.1 Step (1) recommends the use of the optimal target spectrum set among 300 random samplings for record selection and scaling. As a random process, more target generations will result in smaller minimum target residuals. It is important to investigate how many target generations are sufficient for practical purpose. Fig. 6(b) plots the accumulative minimum residuals of the target set against the number of target realizations for populations of 30, 60, 100 and 200. The resulting minimum target residuals can be greatly reduced during the first several hundred random realizations. However, the effort begins to die out as no significant reduction in the minimum target residuals can be made after several thousand realizations. For practical purpose, it is recommended that 300 random target samplings are sufficient based on the results in this example.

Table 2

Summary of the statistical distribution of ground motion characteristics.

Ground motion set	Scale factors	M_w	R_{rup} (km)	D_{5-95} (s)	V_{z30} (m/s)
Scenario	–	7.0	10	14.1 ^a	400
30 records	1.54 (1.28)	6.9 (0.5)	12.8 (8.3)	18.9 (9.9)	410 (169)
60 records	1.75 (1.53)	6.9 (0.5)	14.0 (7.9)	17.9 (10.4)	386 (173)
100 records	2.00 (2.56)	6.9 (0.4)	13.8 (8.0)	16.5 (9.4)	452 (257)
200 records	1.59 (1.51)	6.9 (0.5)	13.3 (7.9)	18.3 (11.9)	426 (261)

Values in bold are averages. Values in parenthesis are the standard deviations.

^a The predicted median of the significant duration is from [21].

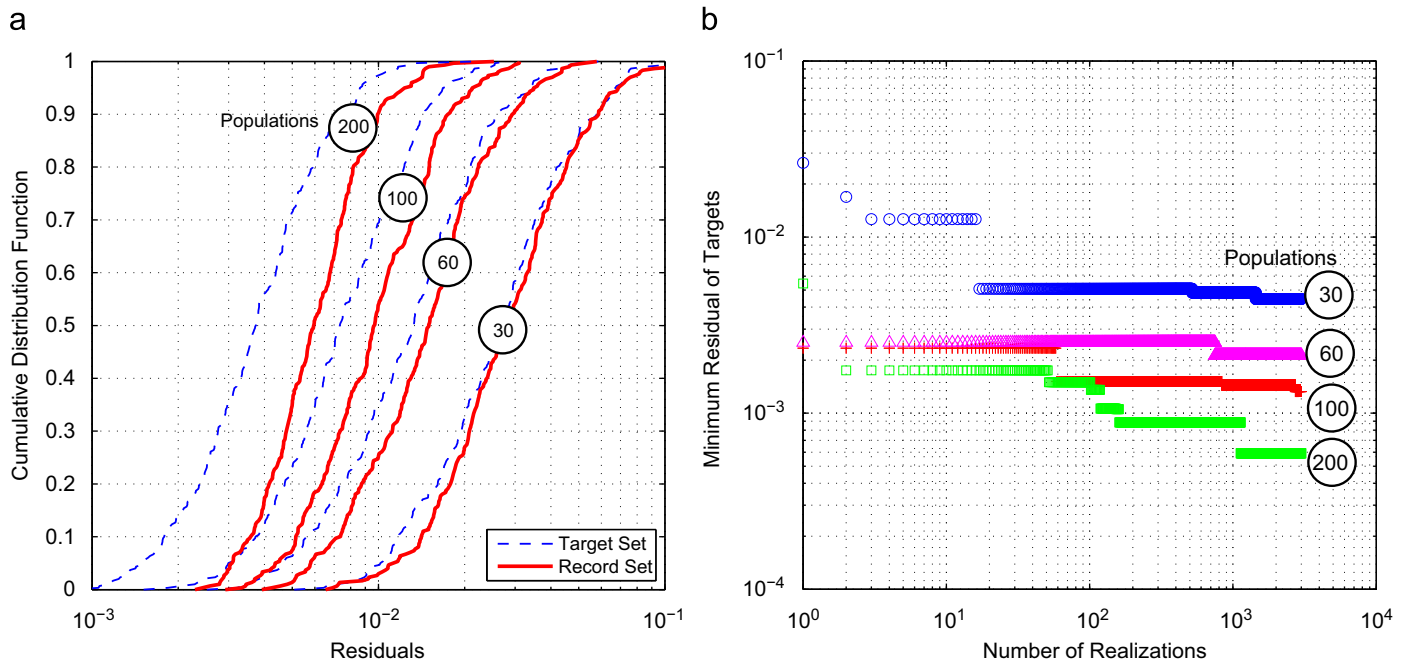


Fig. 6. Convergence test of the record selection and modification algorithm. (a) Residuals distribution (unit: g²), (b) Accumulative minimum residual (unit: g²).

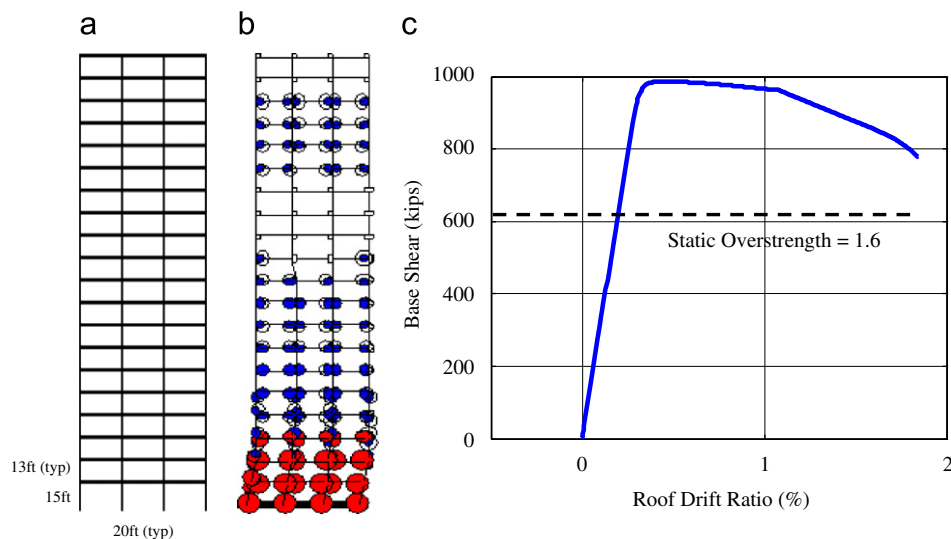


Fig. 7. Structural model layout and characteristic push-over curve adopted from [19]. (a) FEM model, (b) Deformed model and (c) Push-over curve.

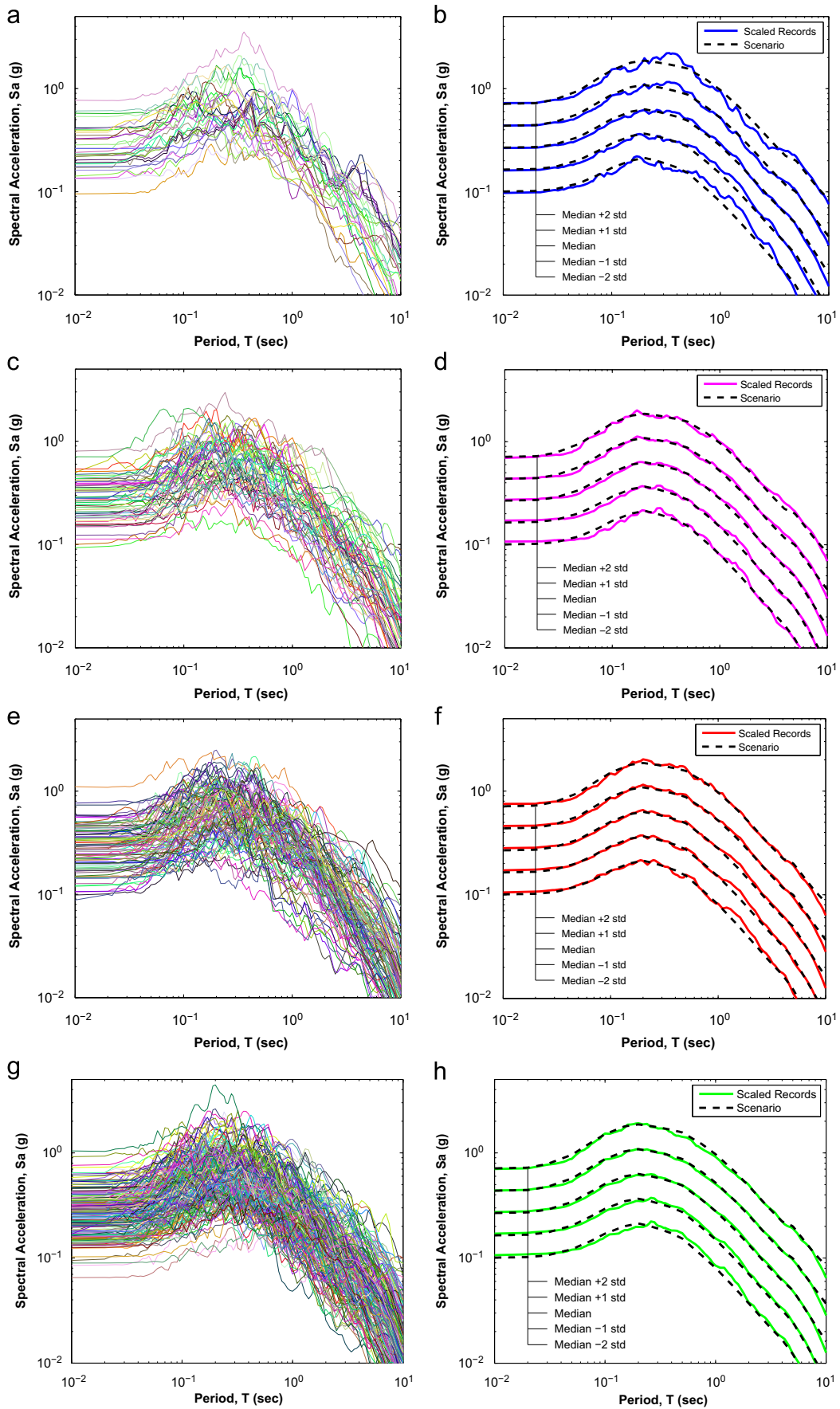


Fig. 8. Spectral distribution of selected ground motions (ground motion set Group 1): (a, b) 30-record set, (c, d) 60-record set, (e, f) 100-record set and (g, h) 200-record set.

4.3. Refined algorithm for global minimum

As shown in the above sections, when the optimal target spectrum set is used to select and scale individual records, it may not necessarily result in a set of scaled records that has the global minimum of the total record residual. To find the scaled set that yields the global minimum residual via Eq. (12), Steps (2)–(4) in Section 4.1 should be repeated for each randomly generated target set, not just for the optimal target set. Yet the computational cost would be significantly increased by 300 times.

Since the target residuals and record residuals are lognormally distributed and linearly correlated, it is not necessary to select and scale records for all target set samplings. Instead, the selection process is needed only if the target residual is smaller than a

specified threshold value δ . Based on tests, the threshold is recommended to be the median minus one standard deviation (in log space) of all target residuals, i.e., $\delta = \exp(\mu(\ln \mathcal{R}_{\text{target}}) - \sigma(\ln \mathcal{R}_{\text{target}}))$. In this case, only 16% of the target set samplings is used to select and scale the record sets. The minimum of the record residuals within the subset will be identified as the global minimum.

The procedure of the refined algorithm is illustrated in Table 1, Step 10. In Fig. 5, the subset of the refined search is highlighted using a box for each case. Only if the residual of the target set falls inside the box shall record selection and scaling be performed. The refined algorithm can identify the global minimum of the record residuals effectively, in the meanwhile, significantly reduces the computational cost by a factor of 10.

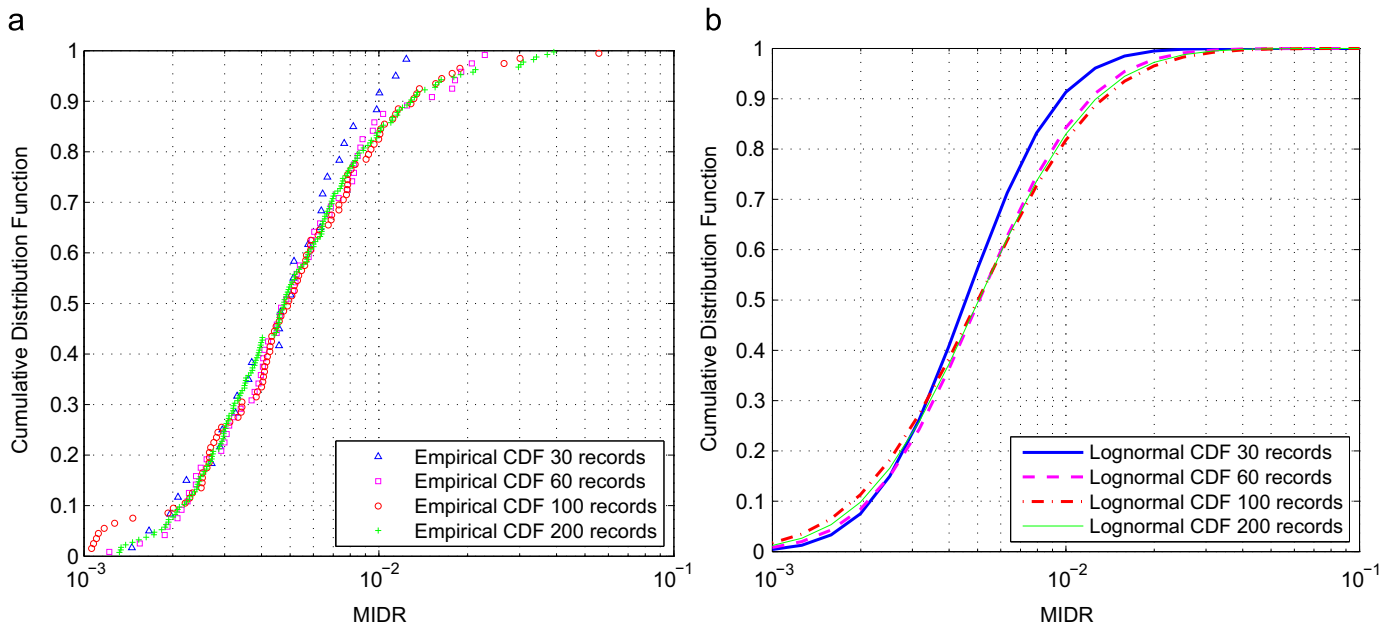


Fig. 9. Comparison of the MIDR CDFs (ground motion set Group 1). (a) Empirical CDFs, (b) Fitted lognormal CDFs.

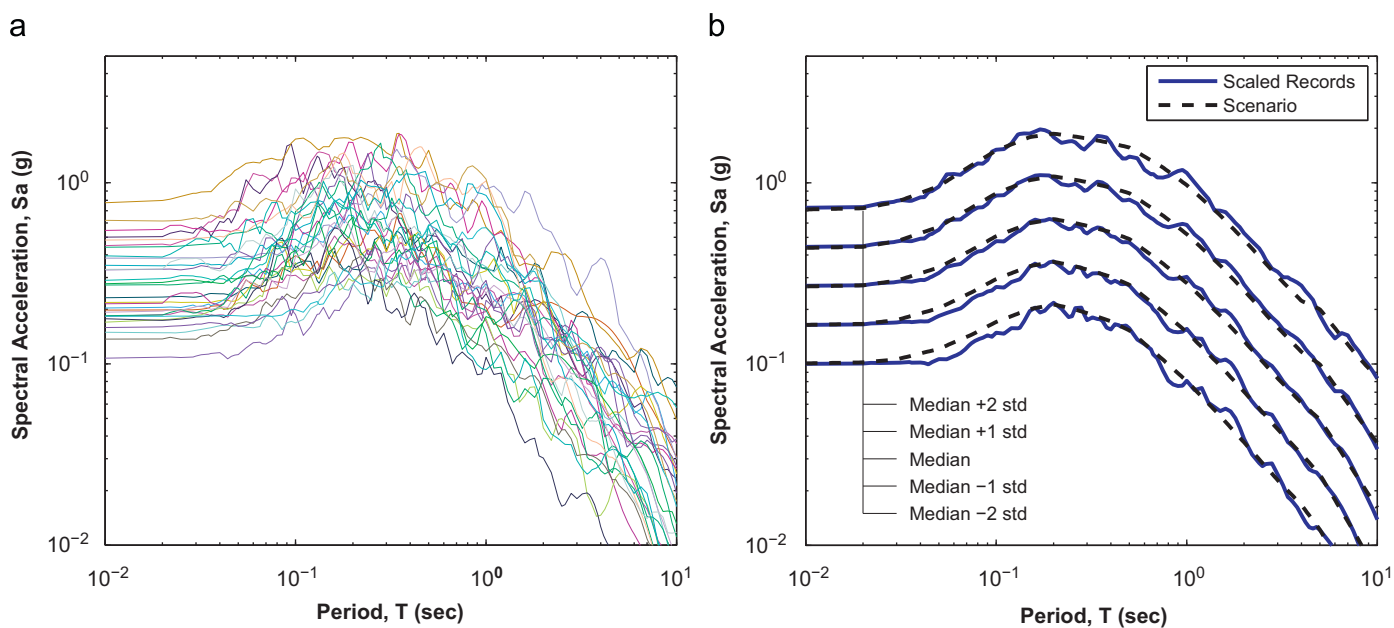


Fig. 10. Spectral distribution for the 30-record set (ground motion set Group 2).

5. Predicting the variability of nonlinear structural response

5.1. The structural model

The efficiency of the GSM scheme is demonstrated in this section to predict the nonlinear response of buildings under a scenario earthquake. The structural model utilized in this study is a modern 20-story reinforced concrete perimeter frame building designed according to the 2003 International Building Code and ASCE7-02. The finite element model was developed in OpenSees [18] by Dr. Haselton (known as Building ID “1020” in [19]). The building represents a typical high-rise ductile frame system with the fundamental period of 2.63 s, and second-, third- and fourth-mode periods of 0.85, 0.46 and 0.32 s, respectively. The same model has been utilized by the PEER GSM Working Group to conduct benchmark tests on various ground motion selection and modification methods (known as Building “C” in [20]).

Fig. 7(a) illustrates the structural layout in the finite element model. The typical bay width of the frame is 20 ft, and the floor height is 13 ft. The reinforced concrete frame is simulated using elasticBeamColumn elements with plastic joints. The deformed model configuration in Fig. 7(b) shows the typical locations of

plastic hinges developed during an earthquake loading, where the outer and inner circles represent the level of plastic rotation demand: when the plastic rotation reaches the limit, the inner circle fills the outer circle (shown as red dots). The strength and stiffness of the building conforms to the expected engineering designs. The base shear versus roof drift ratio is illustrated in Fig. 7(c) based on a static push-over test, where the static overstrength is designed to be 1.6, the design base shear coefficient is 0.044 g, and the ultimate roof drift ratio for collapse (at 20% strength loss) is 0.018. Details of the structural model can be found in [19].

5.2. Selected earthquake records

Same as the examples in Section 4.2, the scenario earthquake for the structural simulation is an event with magnitude $M_w=7$, strike-slip faulting, rupture distance $R_{rup}=10\text{km}$ and $V_{s30}=400\text{ m/s}$. Previous studies have shown that the building response is moderately nonlinear under the scenario earthquake and is sensitive to the second (or higher) mode during the shaking [20]. To take into account the ground motion characteristics besides the response spectrum, the selection bin is limited to records of $M_w=6-8$ and

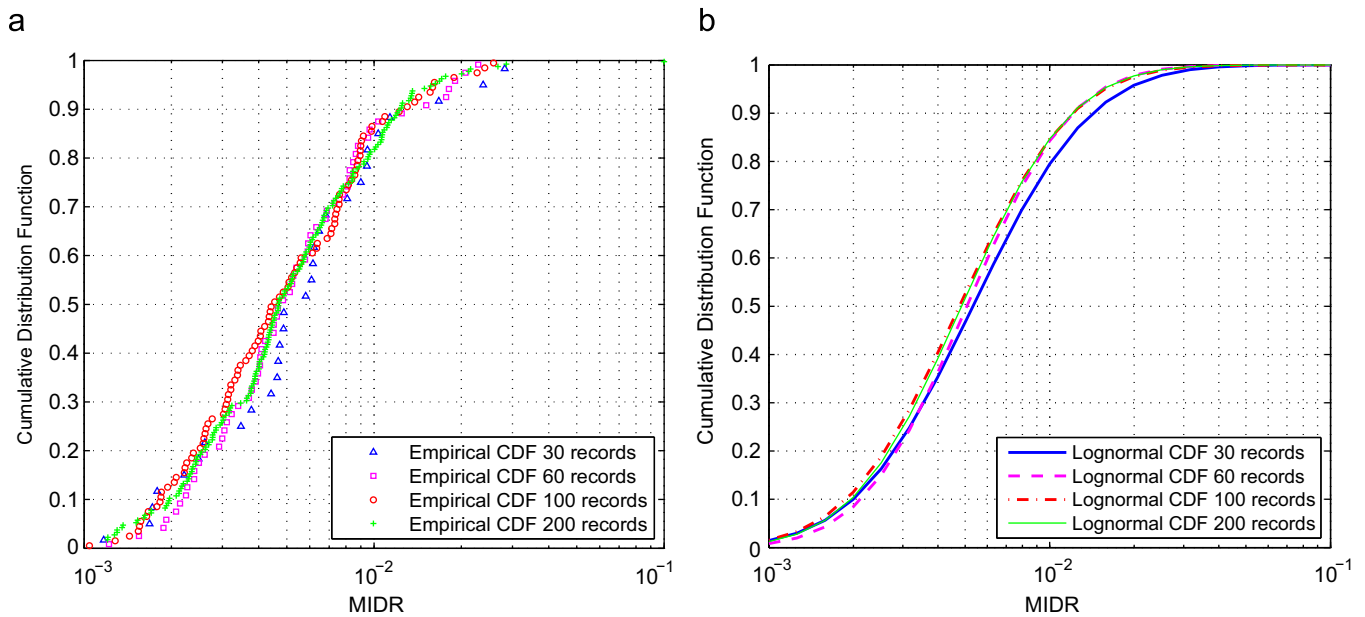


Fig. 11. Comparison of the MIDR CDFs (ground motion set Group 2). (a) Empirical CDFs, (b) Fitted lognormal CDFs.

Table 3
Summary of the estimated lognormal MIDR distributions.

	Populations	MIDR (median)	Standard deviation (in log space)	MIDR (median+1 std.)	MIDR (median+2 std.)
Group 1	30 records	0.0046 (−8%)	0.5757	0.0081 (−21%)	0.0144 (−32%)
	60 records	0.0051 (0.5%)	0.6762	0.0100 (−2.9%)	0.0196 (−7.6%)
	100 records	0.0050 (0%)	0.7610	0.0107 (3.9%)	0.0230 (8.5%)
	200 records	0.0050	0.7176	0.0103	0.0212
Group 2	30 records	0.0053 (8.2%)	0.7653	0.0115 (12%)	0.0246 (14%)
	60 records ^a	0.0051 (4.1%)	0.6762	0.0100 (−2.9%)	0.0196 (−8.8%)
	100 records	0.0048 (−2.0%)	0.7245	0.0098 (−4.8%)	0.0203 (−5.6%)
	200 records	0.0049	0.7361	0.0103	0.0215

Values in parenthesis are the relative errors of each set w.r.t. the 200-record set in each group.

^a The 60-record set is the same in both Group 1 and Group 2.

$\mathcal{R}_{rup} = 0\text{--}30\text{ km}$. Therefore, the size of the data bin is reduced to 758. In this example, the fitness of the record scaling is evaluated over spectral periods ranging from 0.01 to 10 s. No restriction is imposed on the range of scale factors, fault mechanisms, significant duration D_{5-95} or site condition V_{s30} .

Based on the procedures outlined in Section 4, several independent ground motion datasets of populations of 30, 60, 100 and 200 were generated. The first group (called Group 1) of record sets was generated using the procedure in Section 4.1, where the record selection was based on the optimal target spectrum set. The average and standard deviation of magnitude (M_w), rupture distance (\mathcal{R}_{rup}), significant duration (D_{5-95}) and shear wave velocity in top 30 m (V_{s30}) for each selected ground motion set are summarized in Table 2 for inspection. It is known that the nonlinear response of structures is not completely controlled by the response spectrum. Other intensity measures such as the duration measures

need to be checked against the predicted values (e.g. [21]) to avoid any significant bias. In general, the characteristics of the ground motion sets were found to be compatible with the specified earthquake scenario. It was also noted that the same record was allowed to be selected more than once with a different scale factor as long as the scaled spectrum best matches the shape of the target spectrum. In general, a few records will be repeatedly selected in record set of small size (only 2 records were repeatedly selected twice in the 30-record set), while more repeated records may occur in a record set of large size (10 records were repeated twice, and 7 records were repeated three times in the 100-record set). Although it can be easily avoided in the algorithm, repetition may be necessary to generate a record set of large size from a selection bin of relatively small size.

Fig. 8 compares the spectral distribution of the selected ground motion sets against the scenario earthquake (labeled as “scenario”)

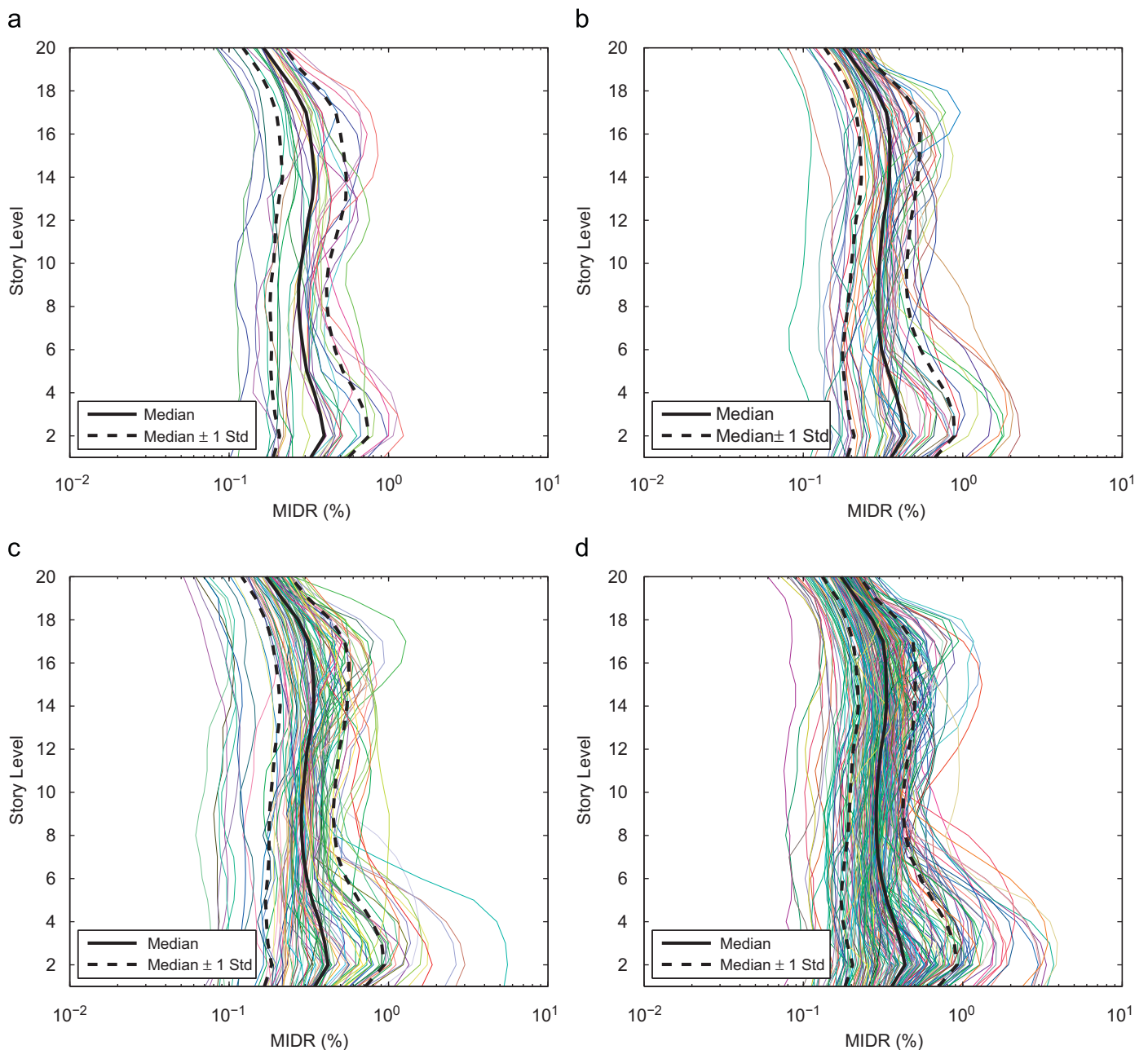


Fig. 12. Distribution of MIDRs for each story (ground motion set Group 1). (a) 30-record set, (b) 60-record set, (c) 100-record set and (d) 200-record set.

for the 30-, 60-, 100- and 200-record sets. Since the GSM procedure selects and scales the records to fit both the median and the standard deviation, these curves closely resembled the prescribed values. While in this example, the fitness of the scaled record spectrum to the target spectrum is specified over the entire period range (0.01–10 s), fitness over a period range of importance can be improved by using weighting functions as mentioned in Step (3) of Section 4.1. Based on the previous studies, the inelastic structural response is sensitive to the response spectral shape over a period range from the third-mode period, T_3 , to twice of the first-mode period, $2T_1$. The period range of importance may be chosen ranging from 0.5 to 5 s for this structure.

5.3. Predicted inelastic structural response

Nonlinear numerical analyses were performed to investigate the seismic response of the 20-story building using the scaled acceleration time-history sets. To simplify the analyses, the maximum interstory drift ratio of all stories (MIDR) was chosen to evaluate the seismic performance. Fig. 9(a) juxtaposes the empirical CDFs for all four ground motion sets in Group 1. It is observed that all empirical CDFs can be well-fitted using lognormal distribution functions, as shown in Fig. 9(b). Very consistent results were obtained for all cases except for the 30-record set, where the MIDRs were slightly underestimated. The underestimation is mainly due to underestimated spectral amplitudes around the first-mode period of 2.63 s, as can be clearly seen in Fig. 8(b). Although 30 records may not be statistically sufficient to represent the spectral variability over a wide range of periods, improvement can be made over a narrower period range of importance from 0.5 to 5 s, as discussed in the previous section.

To further investigate the GSM scheme, a second group (called Group 2) of ground motion sets was generated using the refined algorithm as discussed in Section 4.3. The ground motion datasets in Group 2 achieved the global minimum in record residuals at the expense of higher computational cost than that of Group 1. Group 2 also contains four independent datasets of population 30, 60, 100 and 200. For simplicity, only the 30-record set of Group 2 is shown

in Fig. 10. Compared with the 30-record set of Group 1, the spectral distribution around the first-mode period of the structure is greatly improved for the 30-record set of Group 2. Accordingly, the CDF distribution of the MIDRs is more similar to the record sets of larger populations. A comparison of the empirical CDFs and the fitted lognormal CDFs is illustrated in Fig. 11 for ground motion set Group 2.

Table 3 summarizes the estimated lognormal MIDR distributions for all ground motion sets using the maximum likelihood estimation. In general, the relative errors are reduced when the population of the ground motion sets is increased. For both Group 1 and Group 2, very similar MIDR distributions were obtained from the 60-, 100- and 200-record sets, where the difference is less than 3% for the median MIDRs, and less than 10% for MIDRs at the median +2 standard deviations level.

A comparison of the predicted MIDRs between Group 1 and Group 2 indicates that the refined algorithm does not effectively improve the ground motion sets of large populations (100- and 200-record sets). For example, the relative difference in MIDRs is less than 2.5% between the 200-record sets of the two groups. However, the refined algorithm significantly improved the 30-record set. It is observed that the relative error of MIDRs at the median +2 standard deviations level was reduced from 32% to 15%. Therefore, the refined algorithm is recommended only to improve the smaller population cases. Application of the refined algorithm to large population cases (population > 100) will result in much higher computational cost with little improvement.

Moreover, the distributions of the MIDRs for each story were examined in Fig. 12 for each ground motion set in Group 1. The story-by-story distributions of the MIDRs provide important details for structural optimization. It can be seen that the record sets result in rather consistent MIDRs distributions, especially for the cases of 100 and 200 record populations. It is observed that the MIDRs also approximately follows lognormal distributions for each story. Fig. 13 summarizes the predicted median value and median ± one standard deviation curves for all ground motion sets. Again, consistent results were obtained for all cases, indicating the plausibility of the proposed GSM in capturing the variability of detailed structural response for a specified earthquake scenario.

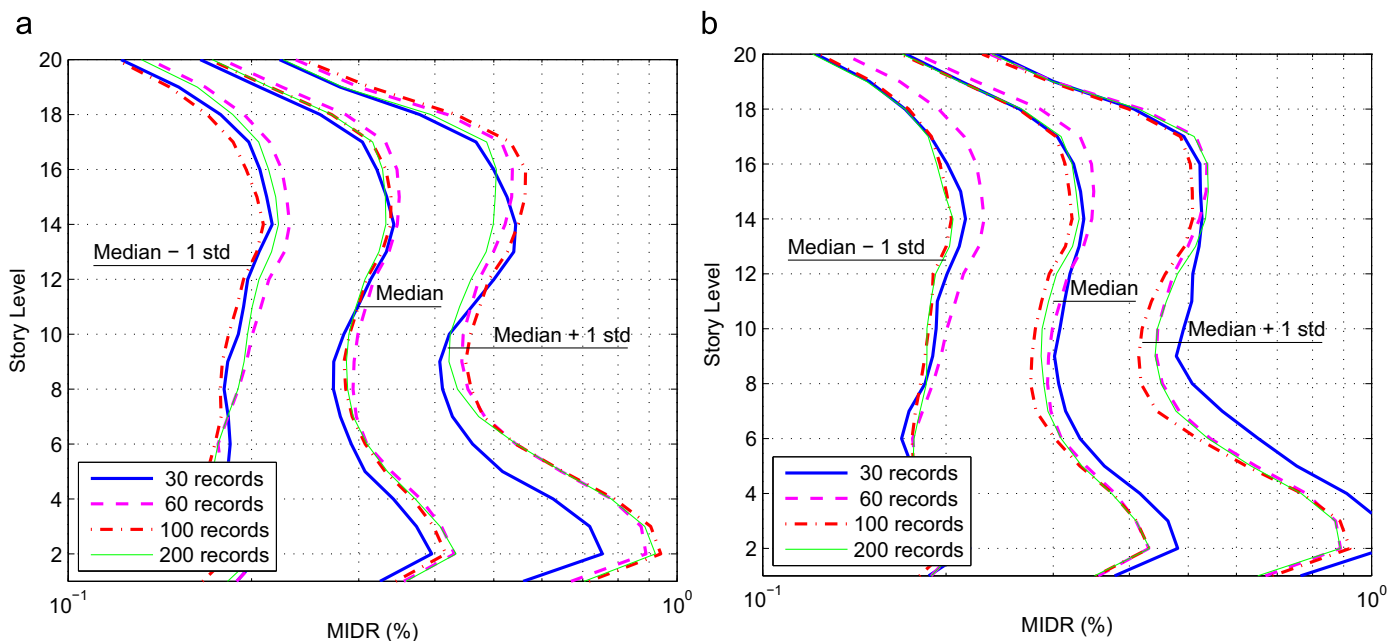


Fig. 13. Summary of the story-by-story MIDR distributions for all ground motion sets. (a) Ground motion set Group 1, (b) Ground motion set Group 2.

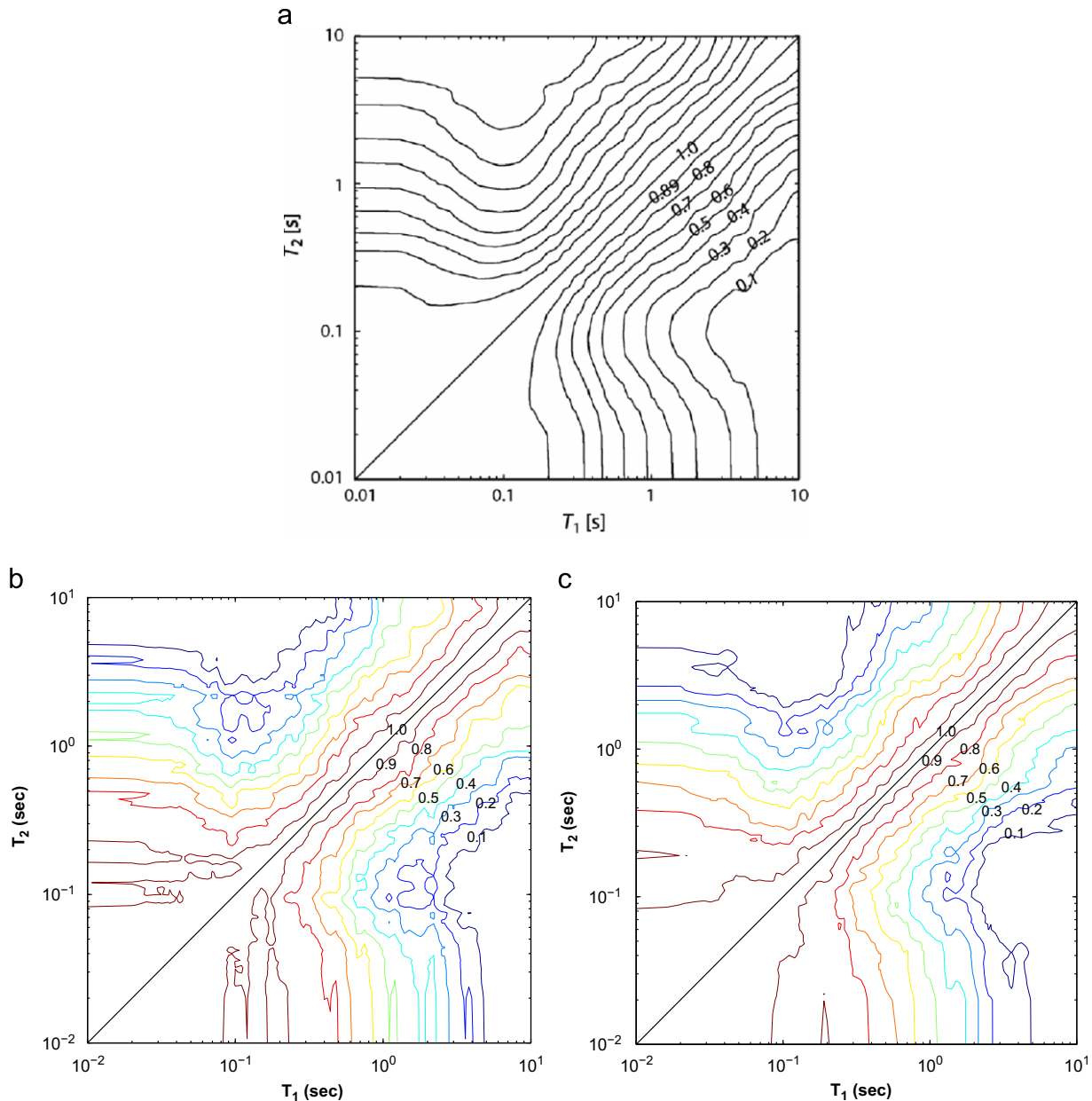


Fig. 14. Contours of correlation coefficients of spectral accelerations: (a) empirical correlation coefficients from NGA dataset, adopted from Ref. [14], (b) realized correlation coefficients from 100-record set and (c) from 200-record set of ground motion set Group 1.

Although detailed structural analysis is beyond the scope of this paper, it is worth pointing out that large MIDRs are localized in the lower 1–5 stories of the building. Participation of higher modes is also important in view of the shapes of MIDR distributions.

As a final check, the correlation coefficients of spectral accelerations obtained from the selected record sets were compared with those regressed from NGA dataset by Baker and Jayaram [14], as shown in Fig. 14. Excellent agreement between these cases indicates that the GMSM method can satisfactorily capture the correlation structure of the scenario earthquake in the scaled record sets, although the GMSM algorithm does not explicitly assess the correlation in the selection and modification process. It is worth pointing out that the realized correlation in Fig. 14(b,c) resembles the one regressed from the strong motion data in Fig. 14(a) more than the smoothed empirical function by Baker and Jayaram in Fig. 1(b), although the correlated target spectra were generated according to the latter.

6. Discussion and Conclusions

In this paper, a new ground motion selection and modification (GMSM) method is proposed to generate a ground motion set that realistically represents the response spectrum characteristics and variability of a scenario earthquake. The proposed algorithm is computational efficient, and the complexity is linear with respect to the size of the database and the population of selected records. By scaling the record spectrum to best match each target spectrum that is randomly generated from a correlated multivariable distribution, the resulting ground motion set can capture the statistical distribution (median, standard deviation and correlation) of the response spectra of a scenario earthquake. It is worth pointing out that the scenario considered throughout the paper conditions on specified earthquake magnitude, rupture distance, type of faulting, site conditions, etc. However, the scenario does not condition on a specific spectral acceleration level, such as the spectral acceleration of the

fundamental period of the structure, $S_d(T_1)$. If this conditional earthquake scenario is considered, the recommended procedure will need to be modified. The modification is straightforward by using the conditional mean spectrum, conditional standard deviation and conditional correlation coefficients in the algorithm to capture the variability of a conditional earthquake scenario.

To demonstrate the efficiency of the proposed algorithm, numerical analyses of a 20-story RC frame structure were performed using seven independent record sets with populations of 30, 60, 100 and 200. The example demonstrated that the proposed method has excellent capacity in capturing the full distribution of interstory drift response under a specified scenario. In particular, a suite of 30 or 60 records selected using the refined algorithm can lead to statistically stable results similar to those obtained from a much larger set, which is quite encouraging for the method to be used in engineering practice. Therefore, the refined algorithm with 30 or 60 ground motions is recommended for practical use in these computationally expensive models. The GSM method provides a direct approach to accurately evaluate the variability of nonlinear seismic response for a specific scenario, which is otherwise difficult to quantify. Therefore, the proposed method has significant implications in performance-based earthquake design.

The record set that preserves the characteristics and variability of response spectra is also helpful to develop predictive models for seismic response of structural and geotechnical systems. Choosing proper intensity measures that have the most predictive powers is the key step in these efforts, and it is still a subject of intense debate. For example, the spectral accelerations (S_a) near the fundamental period of the structure, $S_a(T_1)$, has often been found effective to predict the interstory drift response of first-mode dominate buildings. On the other hand, the peak floor accelerations are more sensitive to the spectral values at high frequencies. The drawback of the traditional methods is that they rely on an accurate estimate of the structural periods. Moreover, contributions from higher frequency modes at periods lower than T_1 or low frequency modes at periods higher than T_1 should be accounted for in inelastic analyses. The problem is particularly important for broadband systems, such as liquefiable soil grounds, Earth slopes and Earth dams. The seismic responses of these nonlinear systems are significantly different from those of buildings in that under strong shaking, the dynamic soil response is affected by ground motion amplitude and frequency contents over a broad range of periods. Spectral accelerations at discrete periods, for example, $S_a(T_1)$ and $S_a(1.5T_1)$ have been used to predict the seismic displacement of soil embankments considering period elongation of a nonlinear Earth system [22]. By preserving the response spectrum characteristics and variability over a wide range of periods, the proposed GSM method will improve the accuracy of the seismic performance evaluation of these broadband systems. Studies are underway to apply the GSM method to these types of systems. The restrictions and limitations of the method will also be explored in future studies.

Acknowledgments

The author would like to thank Dr. Curt B. Haselton of California State University Chico for providing the OpenSees structural models

used in this paper. These models are available through the developer's website at http://myweb.csuchico.edu/~chaselton/research/research_databases/sm_db.php. Discussions with Mr. Maurice Power, Dr. Robert Youngs and Dr. Faiz Makdisi of AMEC Geomatrix Consultants, and comments from two anonymous reviewers have helped to improve the quality of this study. Financial support from the Hong Kong RGC Grants DAG08/09.EG13, DAG11EG03G, and the Li Foundation Heritage Prize Award are greatly appreciated.

References

- [1] Wang G, Power M, Youngs RR, Li Z. Design ground motion library (DGML) (Ver. 2) user's manual, AMEC Geomatrix Consultants, Oakland, California, 2009.
- [2] Abrahamson N. Non-stationary spectral matching program. *Seismological Research Letters* 1992;63(1):30.
- [3] Silva WJ, Lee K. WES RASCAL code for synthesizing earthquake ground motions, Department of the Army, US Army Corps of Engineers, 1987; 121 p.
- [4] Watson-Lamprey J, Abrahamson N. Selection of ground motion time series and limits on scaling. *Soil Dynamics and Earthquake Engineering* 2006;26: 477–82.
- [5] Shantz T. Selection and scaling of earthquake records for nonlinear dynamic analysis of first mode dominate bridge structures. In: Proceedings of the 8th national conference on earthquake engineering, San Francisco, 2006.
- [6] Katsanos EI, Sextos AG, Manolis GD. Selection of earthquake ground motions records: a state-of-the-art review from a structural engineering perspective. *Soil Dynamics and Earthquake Engineering* 2010;30:157–69.
- [7] Shome N, Cornell CA, Bazzurro P, Carballo JE. Earthquakes, records, and nonlinear responses. *Earthquake Spectra* 1998;14(3):469–500.
- [8] Applied Technology Council. Guidelines for seismic performance assessment of buildings (ATC-58 50% draft), <<https://www.atccouncil.org/pdfs/ATC-58-50per centDraft.pdf>>, (accessed December 2009).
- [9] Kottke A, Rathje EM. A semi-automated procedure for selecting and scaling recorded earthquake motions for dynamic analysis. *Earthquake Spectra* 2008;24(4):911–32.
- [10] Campbell KW, Bozorgnia Y. NGA ground motion model for the geometric mean horizontal component of PGA, PGV, PGD and 5% damped linear elastic response spectra for periods ranging from 0.01 to 10 s. *Earthquake Spectra* 2008;24(1): 139–71.
- [11] Chiou B, Youngs RR, Chiou-Youngs NGA. ground motion relations for the geometric mean horizontal component of peak and spectral ground motion parameters. *Earthquake Spectra* 2008;24(1):173–215.
- [12] Abrahamson N, Atkinson G, Boore D, Campbell K, Chiou B, Idriss IM, et al. Comparisons of the NGA ground-motion relations. *Earthquake Spectra* 2008;24(1):45–66.
- [13] Baker JW, Cornell CA. Spectral shape, epsilon and record selection. *Earthquake Engineering and Structural Dynamics* 2006;35(9):1077–95.
- [14] Baker JW, Jayaram N. Correlation of spectral acceleration values from NGA ground motion models. *Earthquake Spectra* 2008;24(1):299–317.
- [15] Chiou B, Power M, Abrahamson N, Roblee C. An overview of the project of next generation of ground motion attenuation models for shallow crustal earthquakes in active tectonic regions. In: Proceedings of the fifth national seismic conference on bridges and highways, San Mateo, California, September 2006.
- [16] Power M, Chiou B, Abrahamson N, Bozorgnia Y, Shantz T, Roblee C. An overview of the NGA project. *Earthquake Spectra* 2008;24(1):3–21.
- [17] Chiou B, Darragh R, Gregor N, Silva W. NGA project strong-motion database. *Earthquake Spectra* 2008;24(1):23–44.
- [18] OpenSees. Open system for earthquake engineering simulation, <<http://open sees.berkeley.edu/>>.
- [19] Haselton CB. Assessing seismic collapse safety of modern reinforced concrete moment frame buildings. PhD dissertation, Stanford University, 2007.
- [20] Haselton CB, editor. Evaluation of ground motion selection and modification methods: predicting median interstory drift response of buildings, PEER report no. 2009/01, Pacific Earthquake Engineering Research Center, University of California, Berkeley, 2009.
- [21] Kempton JJ, Stewart JP. Prediction equations for significant duration of earthquake ground motions considering site and near-source effects. *Earthquake Spectra* 2006;22(4):985–1013.
- [22] Bray JD, Travarasou T. Simplified procedure for estimating earthquake-induced deviatoric slope displacements. *Journal of Geotechnical and Geoenvironmental Engineering* 2007;133(4):381–92.